STUDY OF THERMAL CONDUCTIVITY IN CELLULAR CONCRETES

K. A. N. Silva[1], K. K. B. Pinheiro[2], R. H. P. Lima[3], V. L. G. Teles [4], P. C. C. Gomes[5]

[1]Prof. MS.c Karlisson André Nunes da Silva,
Universidade Federal de Alagoas, Delmiro Gouveia-AL, Brasil
karlisson.silva@delmiro.ufal.br

[2]Eng[a]. Civil Karla Kamila Barros Pinheiro,
Universidade Federal de Alagoas, Maceió-AL, Brasil
karlakamilap@gmail.com

[3]Prof. Dr. Raniere Henrique Pereira Lima,
Universidade Federal de Alagoas, Delmiro Gouveia - AL, Brasil
Raniere.lima@delmiro.ufal.br

[4]Prof. Dr[a]. Vânia de Lourdes das Graças Teles,
Universidade Federal de Alagoas, Maceió-AL, Brasil
vania.teles@ctec.ufal.br

[5]Prof. Dr. Paulo Cesar Correia Gomes,
Universidade Federal de Alagoas, Maceió-AL, Brasil
pgmos@ctec.ufal.br

ABSTRACT

The thermal performance of buildings has been crucial for reducing energy consumption. Concrete, with its good thermal conductivity, is the most widely used material in construction, contributing to increased energy consumption. Lowering concrete density, however, hampers thermal conductivity. The use of lightweight concrete has been recommended for this purpose. Foamed cellular concrete (FCC) is an alternative to achieve lightweight concrete. There is a research gap regarding the thermal conductivity of FCE. In this study, a normal density concrete (NDC) and two FCC's, one with 10% foam (FCC10) and another with 20% foam (FCC20), were analyzed. Specific mass, compressive strength, and thermal conductivity were determined for the concretes. A transient heat conduction method was applied. The results showed that FCC exhibited inferior properties compared to NDC, particularly in thermal conductivity. NDC had a thermal conductivity of 1,75 W/mK, FCC 10 had 1,12 W/mK, and FCC 20 had 0,73 W/mK. When comparing FCC's conductivity to other lightweight concretes, no significant differences were found, highlighting FCC's potential for reduced energy consumption.

KEYWORDS: *Thermal conductivity, density, foamed cellular concrete*

I. INTRODUCTION

The increase in housing worldwide has generated a considerable demand for energy [1]. In the European Union, China, and the United States, heating and/or cooling of buildings consume an average of 37% of the total generated energy [2]. In Brazil, data provided by the Ministry of Mines and Energy, through the National Energy Balance of 2021, show that residential consumption (heating, cooling, lighting, among others) accounts for 26.4% of the demand for the entire national energy production [3]. There is a strong trend in the construction industry towards prefabricated buildings that use concrete as the main material, contributing to the high-energy consumption of buildings [4].
Concrete, due to its good thermal conductivity compared to other building materials, has a direct relationship with the energy consumption of buildings [5]. One favorable solution for reducing the thermal conductivity of concrete is to decrease its density. Concretes with densities lower than 2000

kg/m^3, known as lightweight concrete (LC) [6], have been applied in prefabricated construction systems [7], maritime structures, bridges, and offshore installations [8], presenting lower thermal conductivity than normal density concrete (NDC), 2000 kg/m^3 to 2800 kg/m^3 [6]. The lower thermal conductivity of LC has contributed to better thermal comfort and lower energy consumption [9].

Studies demonstrate that the thermal conductivity coefficient of LC, with density close to 1500 kg/m^3, ranges from 0.65 W/mK to 0.87 W/mK [1], [2], [10], [11]. For densities close to 1700 kg/m^3, other studies have found values between 1.0 W/mK and 1.29 W/mK [2], [11], and [12].

Research on LC, obtained without coarse aggregates, of rocky origin, and using different materials, has managed to decrease the thermal transfer capacity of concrete. LC using aerogel decreased by 20% compared to NDC [13]. LC with rubber aggregates had a thermal capacity reduction between 55% and 25%, respectively, compared to NDC [1], [14]. LC with expanded clay had a thermal reduction 30% lower than NDC [11], [12]. LC using perlite resulted in an 82% decrease in thermal conductivity compared to NDC [1]. In the study of thermal conductivity of LC by inserting fly ash, in all proportions used, there was a reduction in the coefficient of thermal conductivity compared to NDC [15]; The use of expanded polystyrene resulted in up to a 70% decrease in the coefficient of thermal conductivity [16]. Finally, the use of expanded glass instead of aggregates resulted in a 13% increase in the coefficient of thermal conductivity [17].

Lightweight concretes with a foaming agent, called foamed cellular concrete (FCC), are obtained by incorporating foams during their production, promoting the formation of evenly distributed microbubbles in the cementitious matrix [18]. FCC is characterized by its low density [17] and has been applied in prefabricated constructions, contributing to better thermal and acoustic comfort of buildings [6]. However, despite its potential as a material with low thermal conductivity, there is a lack of studies proving the efficiency of FCC.

The determination of concrete thermal conductivity can be obtained by applying a heat source to the material, performed by stationary methods [1]. These involve constant heat transfer using specific equipment, such as the hot box or hot plate [19].

In the study, the thermal conductivity of FCC, obtained with different foam dosages, is determined by a proposed technique, analyzed, and compared with that of NDC. In addition to comparing the thermal conductivity coefficients obtained with those reported in the scientific literature. The results obtained, and the conclusions reached, outline the potential impact of this research in the field of civil engineering and sustainable construction.

II. Work Organization

The article presents the study developed in the following stages: characterization of the materials of NDC and FCC concretes; composition of the concretes (NDC, FCC); production of the concretes and molding, and quantity of test specimens for determination of properties in the hardened state; testing technique, procedures, and mathematical model adopted for determining thermal conductivity; procedures for statistical analysis of the obtained data; analysis of the thermal conductivity coefficients found comparing them to literature values; results and analysis of the specific mass and compressive strength of the obtained concretes.

III. Objectives

The objective of this article is to assess the thermal conductivity coefficient of foamed cellular concretes produced with different densities.

IV. Methodology

4.1. Main characteristics of the materials used

The materials used in the compositions of the concretes were: Portland cement type CPV ARI MAX, which presents a 28-day strength of 60 MPa [20]; density of 2.99g/cm^3 [21]; residue from marble and granite processing (RMGP) [22]; superplasticizer additive (SA) (polycarboxylate) with a specific mass between 1.067 to 1.107g/cm^3 and solids content between 28.5 to 31.5%, according to the manufacturer; air-entraining additive (IA) conventional/synthetic concentrated for foam generation, with a chemical base of sulfated ethoxylated fatty alcohol salt, with solids content of 5%, and density of 1.0 g/cm^3, according to the manufacturer; viscosity-modifying additive (VMA), with an apparent density of 0.4 g/cm^3. The fine natural aggregate (FNA) came from quartz sand with a specific mass of 2.45g/cm^3 and fineness modulus of 2.19. The coarse natural aggregate (CNA) of granitic origin with a specific mass of 2.64 g/cm^3 and maximum aggregate diameter of 9.6 mm.

4.2. Composition, production and molding of concrete

The compositions of normal-density concrete (NDC) and low-density foamed cellular concrete (FCC) are presented in Table 1, indicating the quantity of materials required for the production of 1 m^3 of concrete. The concretes were produced in the Laboratory of Structures and Materials (LEMA) at the Federal University of Alagoas (UFAL).

Table 1: Concrete composition (kg/m^3)

	Type of Concrete			
Materials	Unit	NDC	FCC10	FCC20
Cement	Kg	409.30	673.41	598.41
RMGP		204.70	-	-
Water		184.20	256.29	225.1
SA		6.10	3.14	2.97
FNA		764.30	1009.71	897.2
CNA		764.30	-	-
VMA		-	4.52	9.04
Materials	%	-	10	20
Cement	-	0.45	0.38	0.38

The normal-density concrete (NDC), with a density ranging between 2000 kg/m^3 and 2800 kg/m^3, and the foamed cellular concretes (FCCs), with 10% foam (FCC10) and another with 20% foam (FCC20), have densities lower than 2000 kg/m^3 [23]. It is worth noting that, aiming to enhance result reliability, two productions of each concrete were carried out on two different days, using the same materials, proportions, and procedures. The first production is referred to as NDC 1ª; FCC10 1ª and FCC20 1ª, while the second is called a replica, denoted as NDC R; FCC10 R and FCC20 R. The production of NDC was done in a 120l capacity vertical axis concrete mixer, while FCC10 and FCC20 were produced using a 50l planetary mortar mixer. Prismatic specimens of 10cm x 10cm x 17cm and cubes of 10cm x 10cm x 10cm [24].

4.3 Tests of the concrete in the hardened state

The properties of specific mass were determined on prismatic specimens of 10 cm x 10 cm x 17 cm [25], compressive strength on cubic specimens of 10 cm x 10 cm x 10 cm [26], and thermal conductivity using the method applied to prismatic specimens of 10 cm x 10 cm x 17 cm. For each of the tests, three specimens were produced, totalizing 27 samples for each concrete mix, and resulting in a total of 54 specimens. All concretes were cured in a dry condition until the date of specimen failure, with a curing period of 28 days for specific mass and compressive strength tests and 33 days for the thermal conductivity test.

4.4 Thermal conductivity test

Applied technique follows the transient heat conduction test approach, involving the application of a constant heat source (qk) on the specimen. The method is illustrated in Figure (1a and 1b).

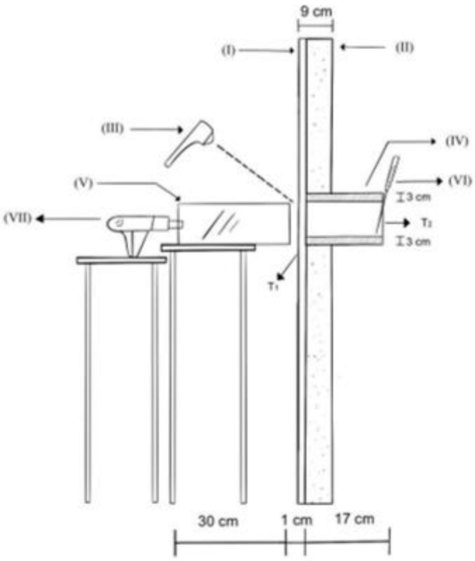

(a)

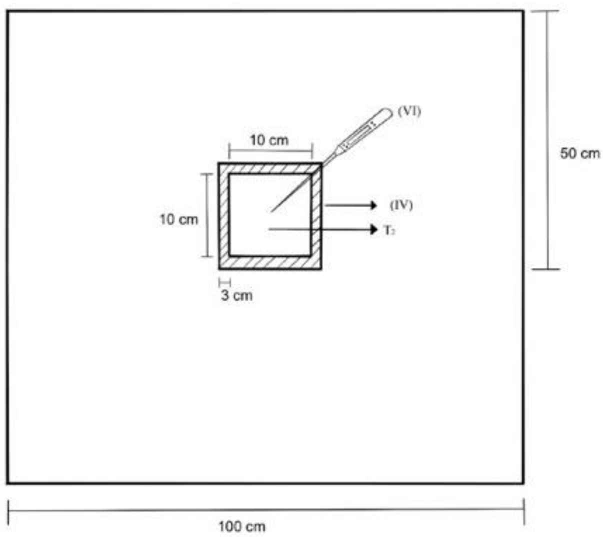

(b)

Figure 1: (a) Side view of the apparatus, (b) opposite view of the apparatus

In Figure (1a), the heat source (*q*), shown in VII, is a constant power thermal blower of 1000W. The flow of hot air is directed through a metal tunnel (V) to the front part of the test specimen (10cm x 10cm) (FACE T1). Subsequently, a thermal shield divided into two parts is positioned. The front part (I) consists of a refractory material with aluminium plates. In the rear part, expanded polystyrene (EPS) board (II) with dimensions of 100 cm x 100 cm x 9 cm is used. This board has a central opening to place the test specimen wrapped in EPS boards (16 cm x 16cm) of 3cm thickness (IV), leaving only the final part of the test specimen (FACE T2) exposed, as shown in Figure 1b. The test specimens were painted black to better absorb all the radiation that reaches them [27]. Temperature measurements on both faces were taken at 5-minute intervals. On FACE T1 of the test specimen, a thermal camera with a measurement range between -30°C to +650°C (III) was positioned, and on FACE T2 of the test specimen, a digital thermometer was attached, with a measurement range varying from -50°C to +300ºC (VI).

To determine the thermal conductivity coefficient (*k*) of the FCC10 and FCC20 concretes, it was necessary to fix the value of a known *k*, for which the value of 1.75 W/mK for NDC was used. This value is applied in concretes with normal density between 2200 kg/m^3 to 2400 kg/m^3 [28]. Additionally, it was necessary to establish the time for which the material enters the steady-state regime (Δt), a behavior evaluated by determining the temperature curves between the parallel faces of the test specimen (T1 and T2), as shown in Figure 4. By substituting the values of k, Δt, ΔT, A, and L into Equation 1 [29], the heat conduction rate (*qk*) in "Watts" was determined for NDC, derived from the average of three test specimens for each production (1st and Replica). This reference *qk* was used to determine the *k* of FCC10 and FCC20 using Equation 1.

$$q_k = \frac{q}{\Delta t} = kA\frac{\Delta T}{L} \qquad \text{Eq. (1)}$$

Once the thermal conductivity coefficients of the FCC10 and FCC20 concretes were determined, they were compared to the values found in the literature.

4.5 Data processing

A statistical analysis using GraphPad Prism 5.01 software with one-way ANOVA and Tukey's multiple comparisons test was applied to evaluate compressive strength and thermal conductivity (*k*). Differences are considered significant when the p-value is less than 0.05, indicating that the results are statistically different. For p-values greater than or equal to 0.05, the results are considered statistically equal. Thus, the obtained results used the average values of three specimens for each test and their standard deviation.

V. Results and Discussions

5.1. Specific Mass

The results of the specific mass test are shown in Figure 2, where the first three columns represent the values from the 1st production, and the last three columns represent the values from the second production or Replica. The NDC concrete exhibited the highest densities 2.38 kg/cm^3 and 2.37 kg/cm^3, respectively. For the lightweight concretes, it was observed that an increase in the air content from 10% to 20% resulted in a decrease in density, a fact evident in both the 1st production and the Replica. The FCC10 ranged from 1.72 kg/cm^3 to FCC20, from 1.49 kg/cm^3 in the 1st production, and from 1.74 kg/cm^3 to 1.53 kg/cm^3 in the Replica, as per the specific mass values [28]. This represents a reduction of 14.36% in the first production and 12.06% in the Replica. Additionally, it was possible to observe that among the values found.

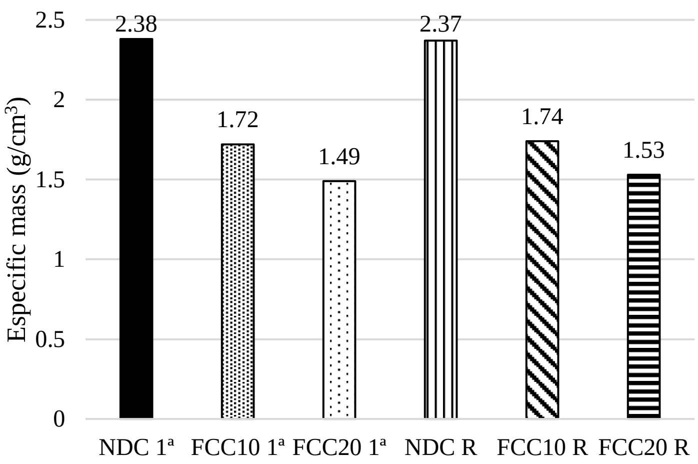

Figure 2: Average specific mass of concrete productions 1ª and Replica

5.2. Compression strength

The average results of compressive strength are presented next (Figure 3). For both the 1st production and the Replica, three different levels of strength were determined. The NDC concretes demonstrated the highest strengths, reaching values of 47.08 MPa and 46.67 MPa, respectively. In contrast, the cellular concretes FCC10 and FCC20 exhibited lower values, with 26.05 MPa and 27.72 MPa for FCC10, and 18.22 MPa and 19.56 MPa for FCC20. These results indicate that the increase in the addition of incorporated air in the concrete leads to a reduction in compressive strength.

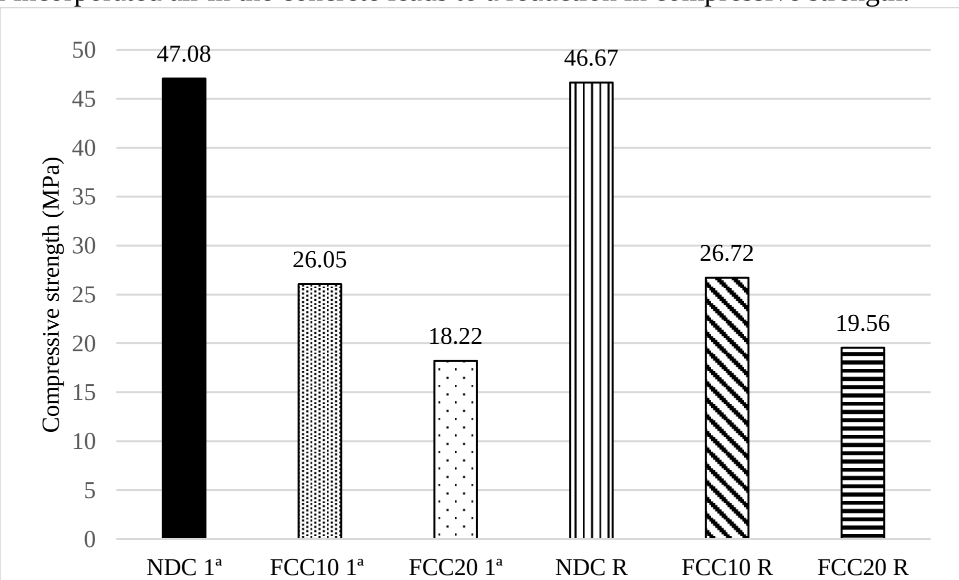

Figure 3: Average value of compression strength for the productions of the concretes 1ª x Replica

Using one-way analysis of variance (ANOVA) and Tukey's multiple comparison test with a 95% confidence level, it was possible to determine that the produced concretes and their replicas exhibit similar characteristics when compared to each other, namely: NDC1ª and NDC R, FCC10 1ª and FCC10 R, and FCC20 1ª and FCC20 R. This implies that the production and concreting procedures were consistent, leading to very close results between the two productions, thereby strengthening the null hypothesis related to the applied treatment, as shown in Table 2.

Table 2: ANOVA with the results of the compression strength test (MPa) (n=3)

Concrete	1ª production	Replica
NDC	47.08 ± 0.93	46.67 ± 1.16
FCC10	26.05 ± 0.54	26.72 ± 1.51
FCC20	18.22 ± 0.44	19.56 ± 1.19
p-valor	> 0.05	> 0.05

5.3. Determination of the time (Δt) to reach steady-state regime

The determination of the time for the test specimens to enter the steady-state regime is shown in the temperature variation curves between the parallel faces T1 (upper curve) and T2 (lower curve), as presented in Figure 4.

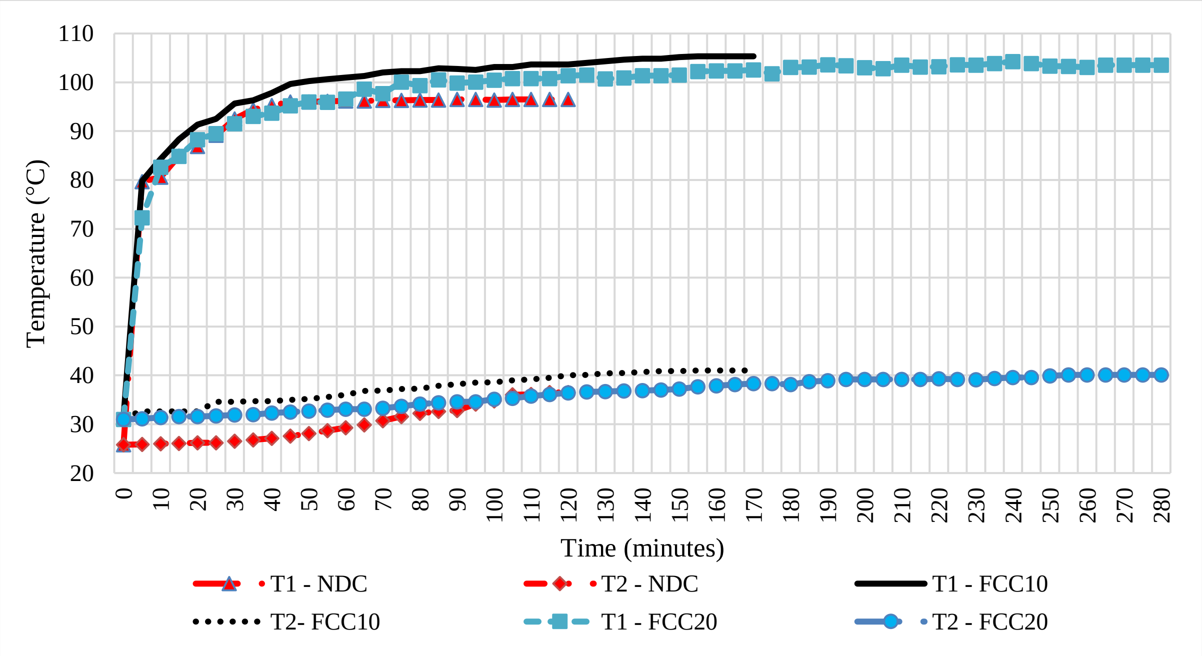

Figure 4: Curvas de ΔT entre as faces T1 e T2 dos concretos ao longo do tempo

The temperature curves of heat transfer between the faces of the test specimen exhibit similar behaviors in reaching the necessary times to achieve steady-state regime. Overall, all concretes presented three well-defined stages, as observed in Figure 4. Initially, there is a rapid heat absorption on face T1, followed by heat transfer between the faces, and finally, the stabilization of temperature between parallel faces T1 and T2. During the first stage, there is a significant temperature change. The test specimens, initially at ambient temperatures around 30°C, reach values between 76°C and 80°C. In the second stage, the heat transfer process by conduction continues gradually. In the third stage, the concretes reach steady-state regime, meaning there is no further temperature variation over time. Thermal equilibrium began approximately at 100 minutes for NDC, while for FCC10, it began around 160 minutes, and for FCC20, around 265 minutes.

5.4 Heat conduction rate (q_k)

With the determination of the value of Δt for the NDC concretes to enter the steady-state regime, and using Equation 1, it was possible to determine the average value of the heat transfer rate ($q_{kaverage}$), presented in Table 3. These values correspond to the average of the observations obtained from three test specimens for each production (NDC 1st and NDC R). As mentioned earlier, determining these values required the adoption of a predicted k, opting for the value of 1.75 W/mK for the NDC. The heat source remained at a constant power of 1000W, and as highlighted in Table 3, the average powers required were 6.43W for NDC 1st and 6.42W for NDC R, respectively. Thus, it was possible to observe that the material is not capable of absorbing all the heat from the source, which can be attributed to the loss of heat by convection between the distance from the heat source and face T1.

Table 3: Average heat transfer rate for concretes of the type NDC.

Concretes	$Q_{kaverage}$ (W)	d_p (J)	C_v (%)
NDC 1ª	6.43	0.22	3.47
NDC R	6.42	0.12	1.95

Table 3 shows that the coefficient of variation Cv (%) among the conducted tests yielded better results for NDC R (1.95), leading to a more precise outcome than NDC 1ª (3.47), even with a very small difference between the values of *qk*.

5.5 Determination of thermal conductivity of FCCs

Once the average *qk* and ΔT for each of the analyzed concretes were determined, it was possible to determine the k for the other concretes by manipulating Equation 1. Table 4 highlights the average values ± dp.

Table 4: ANOVA for thermal conductivity data (W/mK) of concretes (n = 3).

Concretes	1ª production	Replica
FCC10	1.11 ± 0,09	1.13 ± 0.04
FCE20	0.72 ± 0.04	0,74 ± 0.04
p-valor	> 0.05	> 0.05

The one-way analysis of variance (ANOVA) and Tukey's post hoc multiple comparisons test, with a confidence level of 95%, allowed us to conclude that the original concretes and their respective replicas are similar. This finding was obtained by comparing the pairs produced (NDC 1ª and NDC R), (FCC10 1ª and FCC10 R), and (FCC20 1ª and FCC20 R). These results indicate that the production and concreting procedures were consistent, resulting in very similar responses between the two series of concretions, thus corroborating the null hypothesis related to the applied treatment. It is worth noting that the standard deviation equal to zero in the determination of the coefficient (*k*) for NDC is attributed to strategic use to facilitate the determination of the other thermal conductivity coefficients. Once determined, the thermal coefficients of NDC, FCC10, and FCC20 concretes and their replicas were compared to values found in the literature and standards based on specific mass.

5.6 Analysis of thermal conductivity coefficients (*k*) comparing with other authors

The experimentally obtained data were compared with information from articles and standards, as shown in Figure 5. These relate to concretes produced using different production methodologies, types of cement, different water-to-cement ratios, fine aggregates, and various types of additives, such as silica aerogel, rubber aggregate, sintered aggregate, expanded slate, expanded clay, foam, pumice, and expanded perlite. These additives, in controlled proportions, generate concretes with different specific masses. The concretes studied in this research had specific masses ranging from 1498 kg/m^3 to 2378 kg/m³, giving them characteristics of lightweight concretes, with foam content ranging from 10% to 20%, and finally, normal density concrete.

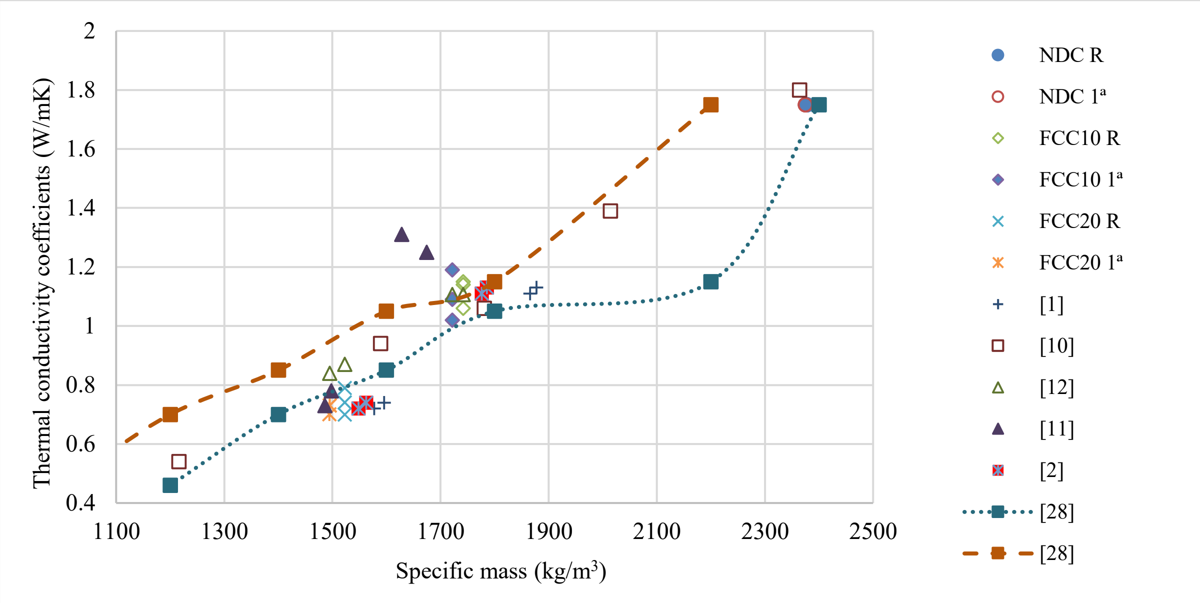

Figure 5: Thermal conductivity of concretes x specific mass.

The correlation between specific mass and thermal conductivity coefficient is presented in Figure 5. It is possible to identify two regions where the values of the specific mass addressed in this article are concentrated. The first is near 1500 kg/m³, where the FCC20 1st and replica concretes are located. The thermal conductivity coefficients for this region varied between 0.64 W/mK and 0.90 W/mK. Lightweight concretes with porosity of up to 20% have thermal conductivity coefficients ranging from 0.61 W/mK to 0.85 W/mK and a mean value of approximately 0.75 W/mK [30]. The second region, where the FCC10 1st and replica concretes are located, is near 1750 kg/m³, presenting values between 0.92 W/mK and 1.2 W/mK. The results demonstrate that reducing the specific mass decreases thermal conductivity, a fact confirmed in the works presented by [1], [10], [11], [12]. This analysis allowed visualizing the trends and groupings of the data, providing a deeper understanding of the relationship between specific mass and thermal conductivity coefficient in the different types of concretes investigated.

VI. CONCLUSIONS

This study undertook an investigation into normal-density concrete (NDC) compared to foam concrete (FCC10 and FCC20), analysing not only changes in specific mass but also their effects on mechanical and thermal properties. The results outlined complex and fundamental relationships between these parameters, providing a broader insight into the performance of these materials. The initial observation of a decrease in the specific mass of foam concretes compared to normal-density concrete was consistent with expectations.

The initial observation of a decrease in the specific mass of foam concretes compared to normal-density concrete was consistent with expectations. The reduced specific mass of FCC10 (1.71 g/cm³) and FCC20 (1.50 g/cm³), compared to NDC (2.38 g/cm³), reflects the introduction of foam cells into the concrete matrix, an essential aspect for applications where weight reduction is critical.

Compression strength was found to be affected by specific mass. The results revealed an inverse correlation, where NDC showed a compression strength of 46.0 MPa, while FCC10 and FCC20 exhibited lower values of 26.0 MPa and 19.5 MPa, respectively. This behaviour suggests that the introduction of foam reduces the concrete's ability to withstand compression loads, highlighting the importance of balancing weight reduction with maintaining structural strength

A distinctive aspect of this research was the analysis of the thermal conductivity of concretes, a critical factor in applications related to thermal insulation. The results revealed a significant influence of

specific mass on thermal conductivity, showing an inverse correlation. NDC, with a fixed thermal conductivity coefficient by standard, had a value of 1.75 W/mK, while FCC10 and FCC20 showed lower values of 1.11 W/mK and 0.72 W/mK, respectively. This relationship suggests that the introduction of foams not only affects mechanical properties but also improves the concrete's ability to act as thermal insulation.
The correlation between the obtained data points to a complex and interconnected relationship between specific mass, compression strength, and thermal conductivity of the studied concretes. The introduction of foams, despite reducing compression strength, offers benefits in terms of weight reduction and improvement of thermal properties. Therefore, when designing structures, the choice between normal-density and foam cellular concretes should be carefully considered, taking into account the specific requirements for each application.

REFERENCE

1. Oktay, H., Yumrutas, R., Akpolat, A. 2015 “Mechanical and thermophysical Mechanical and thermophysical” Construction and Building Materials journal.
2. Gao, T., Jelle, B. P., Gustavsen, A., Jacobsen, S. 2019. "Aerogel-incorporated concrete: An experimental study”. Construction and Building Materials journal.
3. Empresa de Pesquisa Energética (Brasil) (2022). “Balanço Energético Nacional 2021” Ano base 2020 / E. P. E. – Rio de Janeiro:EPE, 2021, pp 292.
4. Neville, A. M. “Tecnologia do concreto” A. M. Neville, J. J. Brooks; tradução: Ruy alberto Cremonini. -2 ed. – Porto Alegre: Bookkman, 2015.
5. Hore, S., Shiuly, A. (2023). “Study of thermal conductivity of different types of alkali-activated concrete: a comprehensive review”. Environment, Development and Sustainability. https://doi.org/10.1007/s10668-023-04118-8.
6. Rossignolo, J. A., “Concreto leve estrutural: Produção, propriedades, microestrutura e aplicações”, 1 ed., São Paulo, Ed. PINI, 2009.
7. Antunes, D., Martins, R., Carmo R. Costa, H., Julio, E. 2021. “A solution with low-cement-lightweight concrete and high durability for applications in prefabrication”. Construction and Building Materials.
8. Sohel, K. M. A., Liew, J. Y. R., Yan, J. B., Zang, M. H., Chia, K. S., 2012. “Behavior of Steel–Concrete–Steel sandwich structures with lightweight cement composite and novel shear connectors. Composite Structures. pp. 3500–3509. http://dx.doi.org/10.1016/j.compstruct.2012.05.023
9. Ibrahim, M., Ahmad A., Barry, M. S., Luai, M., Suhoothi, M. A. C., 2020. “Durability of Structural Lightweight Concrete Containing Expanded Perlite aggregate. Structures and Materials. https://doi.org/10.1186/s40069-020-00425-w.
10. Sacht, H. M., Rossignolo, J. A., Santos, W. N. 2010. “Avaliação da condutividade térmica de concretos leves com argila expandida”. Revista Matéria, v. 15, n. 1, pp. 031 – 039.
11. Gomes, M. G. Flores-Colen, I. Manga, L.M. Soares, A. Brito, J. 2017. “The influence of moisture content on the thermal conductivity of external thermal mortars”. Construction and Building Materials http://dx.doi.org/10.1016/j.conbuildmat.2016.12.16.
12. Real, S., Bogas, J. A., Gomes, M. G., Ferrer, B. 2016. “Thermal conductivity of structural lightweight aggregate concrete”. Magazine of Concrete Reseach, 68(15), 798-808. http://dx.doi.org/10.1680/jmacr.15.00424
13. Strzałkowski, J., Garbalinska, H., 2016. “Thermal and strength properties of ligtweight concretes with the addition of aerogel particles. Advances in Cement Researrch. ICE Publishing: ALL rights reserved, pp. 567-575. http://dx.doi.org/10.1680/jadcr.16.00032
14. AbdulAmeer, Osama.L 2018. “Assessment the thermal properties lightweight concrete produced. MATEC web of conferences. https://doi.org/10.1051/matecconf/201816202027
15. Habsya, C., Diharjo K., Setyono P., Satwiko P. 2018. Physical, mechanical and thermal properties of lightweight foamed concrete with fly ash. “2nd Nommensen International Conference on Technology and Engineering”. IOP Conf. Series: Material Science and Engineering 420. doi:10.1088/1757-http://dx.doi.org/10.5755/j01.sace.4.5.4188
16. Demirboga, R., Kan, A., 2021. “Thermal conductivity and shrinkage properties of modified waste polystyrene aggregate concretes. Construction and Building Materials. pp 730- 734. http://dx.doi.org/10.1016/j.conbuildmat.2012.04.105
17. Bumanis, G., Bajare, D., Korjakins, A. 2013. Mechanical and Thermal Properties of Lightweight Concrete Made from Expanded Glass. Journal of sustainable architecture and civil engineering No. 2(3). https://doi.org/10.1016/j.conbuildmat.2020.122153.

18. Tayeh, B., Hakamy, A., Amin, Mohamed., Agwa, I. S. 2022. "Effect of air agent on mechanical properties and microstructure of lightweight geopolymer concrete under high temperature". Case studies in construction materials 16 (e00951).
19. Asadi, I., Shafigh, P., Hassan, Z. F. Bin Abu., Mahyuddin, N. B. 2018. "Thermal conductivity of concrete – A review". Journal of Building Engineering, 20, 81–93. https://doi.org/10.1016/j.jobe.2018.07.002
20. ASSOCIAÇÃO BRASILEIRA DE NORMAS TÉCNICAS. NBR 7215/2019: Cimento Portland – Determinação da resistência à compressão de corpos de prova cilíndricos. Rio de Janeiro, 2019.
21. ASSOCIAÇÃO BRASILEIRA DE NORMAS TÉCNICAS. NBR 16605/2017: Cimento Portland e outros materiais em pó – Determinação da massa espcífica. Rio de Janeiro, 2017.
22. ASSOCIAÇÃO BRASILEIRA DE NORMAS TÉCNICAS. NBR 10004/2004: Resíduos solídos classificação. Rio de Janeiro, 2004.
23. ASSOCIAÇÃO BRASILEIRA DE NORMAS TÉCNICAS. NBR 8953: Concreto para fins estruturais – Classificação pela massa específico, por grupos de resistência e consistência. Rio de Janeiro, 2015.
24. COMITÉ EUROPEU DE NORMALIZAÇÃO NP EN 12390-1, 2003: Ensaio do betão endurecido – forma, dimensões e outros requisitos para ensaios de betão e moldes. Portugal.
25. ASSOCIAÇÃO BRASILEIRA DE NORMAS TÉCNICAS. NBR 9778/2005: Argamassa e concretos endurecidos – Deterinação de absorção de água, índice de vazios e massa específica. Rio de Janeiro, 2005.
26. COMITÉ EUROPEU DE NORMALIZAÇÃO NP EN 12390-3, 2009: Ensaio de betão endurecido – Parte 3, resistência à compressão de provetes.
27. R. G. Campiteli, R. G. Morelli, M. R. 2016. "Effect of iron chromite coating addition in the emissivity of a high alumina refractory castable". Cerâmica, pp. 224-229. http://dx.doi.org/10.1590/0366-69132016623632009.
28. ASSOCIAÇÃO BRASILEIRA DE NORMAS TÉCNICAS. NBR 15220-2, 2005: Desempenho térmico de edificações parte 2: Métodos de cálculo da transmitância térmica, da capacidade térmica, do atraso térmico e do fator solar de elementos e componentes de edificações. Rio de Janeiro.
29. Incropera, F. P., Dewitt, D. P., Bergman T. L., Lavine A. S., "Fundamentos de transferência de calor e de massa. Editora LTC, 2008, ISBN 978-85-216-1548-2, Rio de Janeiro.
30. Chen, J., Wang,H., Xie, P., Najm, H., 2019. "Analysis of thermal conductivity of porous concrete using laboratory measurements and microstructure models". Construction and Building Materials,pp 90-98. https://doi.rg/10.1016/j.conbuildmat.2019.05.120

Author

Karlisson André Nunes da Silva: Professor at the Universidade Federal de Alagoas (UFAL), Campus do Sertão. He holds a Master's degree in Civil Engineering with a phase in structures for UFAL (2011). Currently he is doing doctorate in the post-graduation program in materials (PPGmat – UFAL). He have experience in the following topics: repurposing of construction waste and demolition, structural calculation.

Karla Kristina Barros Pinheiro: She is a civil engineer graduated from UFAL (2023) and also holds a degree in Electronics from the Federal Institute of Alagoas (IFAL). She has experience in the field of self-compacting concrete production.

Raniere Henrique Pereira Lira: He holds a Ph.D. in Chemical Engineering from the Federal University of Campina Grande (2020). Currently, he is a Higher Education Professor in the field of Transport Phenomena and Transfer at the Federal University of Alagoas, Campus do Sertão. He has experience in the area of Chemical Engineering, with emphasis on Membrane Separation Processes.

Paulo Cesár Correia Gomes: He is a full professor at UFAL, holds a bachelor's degree from UFAL (1990), with a master's degree from the Federal University of Rio de Janeiro in 1995, a doctorate from the Universitat Politècnica de Catalunya in 2002, and postdoctoral studies from the Polytechnic School of the University of São Paulo in 2015. He teaches courses in the basic, professional, and specific cores. His research focuses on Civil Engineering, with an emphasis on concrete technology, special concretes, and unconventional materials. Additionally, he engages in extension activities at the Laboratory of Structures and Materials at the Technology Center of UFAL.

Vânia de Lourdes das Graças Teles: She holds a Ph.D. in Sciences – Analytical Chemistry from UFMG (2021). She is a professor at the Center for Technology at the Federal University of Alagoas. She has experience in the area of Instrumentation for Chemistry Teaching, material characterization, and Analytical Chemistry, with expertise in topics such as digital technologies in teaching, synthesis, and characterization of nanocomposites, among others